

Lawrence Berkeley National Laboratory

Recent Work

Title

DEVELOPMENT OF A HELIUM-FILLED STREAMER CHAMBER SYSTEM

Permalink

<https://escholarship.org/uc/item/0qc8p7v3>

Authors

Perez-Mendez, Victor
Stetz, Albert W.

Publication Date

1968-05-27

UGRL-16894

University of California

Ernest O. Lawrence
Radiation Laboratory

~~DIFFUSION-INDUCED DEFECTS IN SILICON - PART I~~

TWO-WEEK LOAN COPY

This is a Library Circulating Copy
which may be borrowed for two weeks.
For a personal retention copy, call
Tech. Info. Division, Ext. 5545

Berkeley California

DISCLAIMER

This document was prepared as an account of work sponsored by the United States Government. While this document is believed to contain correct information, neither the United States Government nor any agency thereof, nor the Regents of the University of California, nor any of their employees, makes any warranty, express or implied, or assumes any legal responsibility for the accuracy, completeness, or usefulness of any information, apparatus, product, or process disclosed, or represents that its use would not infringe privately owned rights. Reference herein to any specific commercial product, process, or service by its trade name, trademark, manufacturer, or otherwise, does not necessarily constitute or imply its endorsement, recommendation, or favoring by the United States Government or any agency thereof, or the Regents of the University of California. The views and opinions of authors expressed herein do not necessarily state or reflect those of the United States Government or any agency thereof or the Regents of the University of California.

sub. to Journal
of Applied Phys.

UCRL-16894

UNIVERSITY OF CALIFORNIA
Lawrence Radiation Laboratory
Berkeley, California
AEC Contract W-7405-eng-48

DIFFUSION INDUCED DEFECTS IN SILICON - PART I

E. Levine, J. Washburn and G. Thomas

May 1966

DIFFUSION INDUCED DEFECTS IN SILICON - PART I

E. Levine, J. Washburn and G. Thomas

Inorganic Materials Research Division, Lawrence Radiation Laboratory
and Department of Mineral Technology, College of Engineering,
University of California, Berkeley, California

ABSTRACT

Dislocations introduced into the surface layers of silicon crystals by boron and phosphorus diffusion treatments of the type used in device manufacture were studied by transmission electron microscopy. Edge dislocation arrays were found for $\{110\}$ and $\{111\}$ surface orientations as was the case for previous observations on $\{100\}$ specimens. The maximum density of dislocations was located at a depth corresponding to the steepest solute concentration gradient. The observations suggest that the glide mechanism for motion of edge dislocations into a crystal, previously proposed for diffusion into a $\{100\}$ surface, does not operate for a $\{111\}$ surface orientation. Most of the edge dislocations making up the accommodation network for the latter orientation apparently had moved into the crystal nonconservatively.

INTRODUCTION

Solid state devices which have been made by a shallow diffusion of boron or phosphorus into the surface of a silicon wafer often contain an array of dislocations that partially relieves the solute contraction stress. These dislocations have been revealed by etch pit, ^(1,2) x-ray ⁽³⁾ and electron microscopy ⁽⁴⁻⁶⁾ techniques. The previous electron microscopy observations were made on phosphorus diffused samples for which the dislocation array is less than 10^{-4} cm from the original surface. Washburn et. al. ⁽⁵⁾ observed phosphorus induced dislocations in {100} wafers and suggested a glide mechanism for motion of the dislocation array into the crystal. Dislocation networks in {111} wafers were studied by Jaccodine ⁽⁴⁾ and Joshi and Wilhelm. ⁽⁶⁾ The latter authors also concluded that the dislocations had moved into the crystal by glide on the inclined {111} planes.

It is the purpose of this paper to report the results of detailed observations on phosphorous diffused {111} and {110} wafers and to compare the dislocation networks to those that are introduced by boron diffusion. The use of stereo techniques in conjunction with diffraction contrast experiments permitted a more complete characterization of the dislocation arrays than those made in previous studies.

EXPERIMENTAL

Czochralski grown melt doped p type single crystal silicon was used as the starting material for the phosphorus diffused samples and n type silicon for the boron diffusion. Slices in the {111} or {110} orientation and approximately 1mm thick and 25 mm. diameter were cut from these

crystals. Wafers were lapped and chemically polished to a final thickness of 200 microns, thus removing all mechanical damage. They were then symmetrically diffused in a tube type furnace. The boron samples were diffused at 1200°C using a B_2O_5 source, and then air cooled to room temperature. The surface concentration of boron as determined by four point probe measurements was 2.5×10^{20} at/cm⁻³. The boron diffused samples were then sectioned by anodic oxidation⁽⁷⁾ and a solute profile was obtained down to the pn junction. Samples for electron microscopy were prepared for several different depths within this solute profile. Phosphorous diffused samples were prepared using a P_2O_5 source at 1000°C for 15 minutes. The resultant surface concentration of phosphorus was 3×10^{20} at/cm⁻³.

Because previous authors had examined the dislocation density at various levels for phosphorus diffused samples this was not repeated. Since the maximum density occurs near the surface, only this level was examined. The main purpose of these observations was to establish the predominant mode of dislocation motion in {111} and {110} diffused wafers. The wafer used for {110} diffusion was prepared for an investigation on the defect structure associated with double diffused structures (for details see Part II), however, the dislocation configurations which result from the phosphorus diffusion of the emitter should be characteristic of diffusion induced dislocations in {110} oriented wafers.

Thinning for electron microscopy was carried out from one side only with the side of interest protected with Apezion wax. Slices were prepared for transmission electron microscopy as described previously.⁽⁸⁾

A Siemens electron microscope operated at 100KV and fitted with

a Gatan double tilting stage was used. Stereo pairs were made by taking two micrographs of the same area before and after a tilt of about 7° about an axis perpendicular to the $\{220\}$ reflecting plane. By making use of the corresponding $\{220\}$ kikuchi band similar two beam contrast conditions could be achieved for the two micrographs. The 220 reflections were chosen so that the maximum number of dislocations would be in contrast. In most stereo pairs this included all of the dislocations present in that area of the specimen.

The method of preparation resulted in a specimen 1-2mm in diameter, the periphery of which was thin enough to obtain many thin areas. This type of specimen made it possible to survey large areas of the wafer.

Burgers vectors of all the dislocation segments in a given area were determined using twice the number of reflections that are normally necessary. A kikuchi map⁽⁹⁾ facilitated rapid changes in orientation to obtain pre-selected diffraction vectors before contamination of the specimen occurred. To ensure simple two beam diffraction contrast conditions, photographs were taken in dark field by tilting the gun or in bright field after contours were checked in aperture dark field. A series of photographs were often required as the $s=0$ condition was swept across the field of view. The photographs used as illustrations are those for which there was little long range lattice curvature within the observed area. Therefore, dislocations are in similar contrast over wide areas. The reflections used in $\{111\}$ foils were $02\bar{2}$, $20\bar{2}$, $\bar{2}20$, $1\bar{1}\bar{3}$, $1\bar{3}1$ and $\bar{3}11$, by appropriate tilting of the sample.

RESULTS AND DISCUSSION

The solute profile obtained by sectioning of the boron diffused samples is shown in Fig. 1. The levels which were investigated by electron microscopy are indicated on the curve.

Specimens 3a and 5b which were obtained near the diffused surface did not have any visible defect structure. This is the depth at which the maximum dislocation density occurred in phosphorus diffused specimens. Specimen 4a was the first to have an observable dislocation content. A typical field of view contained one or more inclined dislocations that usually cut through the foil from top to bottom surface.

Specimen 3b was taken at a depth near the maximum concentration gradient and had the greatest dislocation density of all the specimens examined in this series. As can be seen from Fig. 2 many of the dislocations at this level cut through the foil from top to bottom surface. The parts of steeply inclined dislocations that are near one of the foil surfaces often appear in dotted contrast as expected. Dislocations were distributed in a 3 dimensional network rather than lying in a plane parallel to the diffusion front as is clearly revealed by the stereo pair, Fig. 3. Several areas at the same depth were examined in this way. In Fig. 4, which shows the same area as that in Fig. 3, Burgers vectors have been determined by diffraction contrast experiments. They are shown for all segments by short lines parallel to their projections onto the $\{111\}$ foil plane. The six possible projections are indicated by the tetrahedron which is drawn on the print. Most dislocations were near edge orientation and had one of

the three Burgers vectors that were parallel to the diffusion front. Those dislocation lines in Fig. 4 that have one of the three inclined Burgers vectors are indicated by lines with arrows. Examination of the stereo pictures along with the complete Burgers vector assignment leads to the conclusion that it would have been difficult for this array to have formed primarily by glide motion of dislocations having inclined Burgers vectors and their recombination to form the edge array. It appears likely that most of the dislocations have moved into the crystal by nonconservative or climb motion and that only occasionally has a dislocation with one of the three inclined Burgers vectors moved conservatively into the crystal. Further support for this conclusion is also afforded by the fact that the steeply inclined dislocations seen at depths between the main array and the surface were also edge dislocations having one of the three predominant Burgers vectors.

The final level examined was located near the p-n junction (5a). At this level very few dislocations were observed. Those that were found also had one of the three Burgers vectors parallel to the foil surface. Some were u shaped with both ends emerging at the same surface of the foil.

Electron microscope observations were also made on (111) silicon wafers which were phosphorus diffused as described previously. These observations were made only within one foil thickness of the original surface as this is where the maximum density of dislocations had been found previously. In these specimens the dislocation distribution was quite uneven. Areas of relatively high dislocation density such as

that shown in Fig. 5 were separated by spaces about 5μ across within which few dislocations were present. Surface precipitates were also present only in the areas where patches of dislocations were found. Again these dislocations were almost all near edge orientation and had Burgers vectors that were in the $\{111\}$ plane parallel to the surface. The stereo pair in Fig. 6 again suggests that the dislocations have moved into the specimen by climb. In most areas dislocation half loops corresponding to two of the three coplanar Burgers vectors appeared to have climbed into the crystal. Segments having the third Burgers vector were then formed where intersection occurred. At A, B and C dislocations have come close enough to begin to interact and at D, E, F and G short segments having the third Burgers vector have been formed (Fig. 5). Dislocations having inclined Burgers vectors were never observed in the phosphorus diffused $\{111\}$ foils. These conclusions differ from those of Joshi and Wilhelm⁽⁶⁾ who suggested that dislocation motion occurred by glide on the inclined $\{111\}$ planes in $\{111\}$ specimens.

The precipitation on the surface shown in Fig. 5 appears to be associated with the dislocation patches but individual precipitates generally could not be associated with a particular dislocation segment. Schmidt and Stickler⁽¹⁰⁾ have observed similar precipitation in phosphorus diffused samples and have identified them as silicon phosphide with an orthorhombic structure. Although precipitate reflections were observed, they were not of sufficient intensity or number to perform an analysis. The one weak spot observed indicated a lattice spacing of 6.8\AA . The plane corresponding to this spacing was parallel to the

(111) plane of the silicon matrix. This spacing agrees with the (100) spacing of the orthorhombic structure proposed by Schmidt and Stickler. The precipitate is probably in the form of thin platelets on the (111) planes. In dark-field the black side of the black white contrast at precipitates was always in the same direction as \bar{g} indicating an interstitial type of strain field. A study of precipitation in diffused foils will be reported as part II of this paper and thus will not be discussed further here.

Dislocations due to boron diffusion have been very difficult to observe by electron microscopy because they exist at many foil thicknesses away from the original surface (about 2/3 of the way to the pn junction). Therefore with random sectioning there is little chance of finding the array. Dislocations would always be expected at or near the maximum concentration gradient so as to best accommodate the misfit between the contracted diffused region and the matrix. The positions of the arrays for both boron diffusion and phosphorus diffusion are consistent with the solute profiles. In the case of boron diffusion the profile after the particular treatment employed (Fig. 1) had a rather broad plateau near the original diffusion surface and thus no appreciable concentration gradient. The only dislocations found in this area were steeply inclined segments of dislocations which extended to the main network located deeper in the wafer. The solute profile for phosphorus diffusion obtained by Joshi and Wilhelm⁽⁶⁾ does not have this broad plateau but has a small, but probably significant, concentration gradient near the surface. This gradient may be even steeper than indicated, as four point probe readings were taken at the surface and

at 2500A°, but not in the critical area in between. This area is where the maximum density of dislocations is observed.

Dislocation networks produced by diffusion into a (110) surface were also investigated. A typical area is shown as a stereo pair in Fig. 7 and the Burgers vectors are indexed in Fig. 8. The network contains long edge dislocation segments lying approximately parallel to [001] with Burgers vectors $a/2 [1\bar{1}0]$. These relax the contraction stresses in the $[1\bar{1}0]$ direction. Because $a/2 [1\bar{1}0]$ is the only Burgers vector that lies in the (110) plane the contraction stress in the [001] direction must be relaxed by dislocations having the inclined Burgers vectors $a/2 [10\bar{1}]$, $a/2 [0\bar{1}1]$, $a/2 [10\bar{1}]$ and $a/2 [0\bar{1}1]$. Two or more of these Burgers vectors are represented in the distorted hexagonal network. Frequently two or three dislocations of the same Burgers vector but not lying at the same depth tended to line up one above the other as would be expected because of their predominantly edge character (e.g. at A, Fig. 8).

Dislocations having one of the four inclined Burgers vectors can glide into the specimen on (111) and $(1\bar{1}\bar{1})$ in predominantly edge orientation or on the slip planes that lie at right angles to the surface $(1\bar{1}\bar{1})$ and $(\bar{1}11)$, in predominantly screw orientation. Both modes appear to be represented in Fig. 7. The dislocations with Burgers vector parallel to the plane of the surface, $a/2 [1\bar{1}0]$, can only be introduced in edge orientation by recombination of two of the dislocations of inclined Burgers vector i.e. $1/2 [10\bar{1}] + 1/2 [0\bar{1}1] \rightarrow 1/2 [1\bar{1}0]$, or by climb.

The previous observations on specimens with (100) surface

orientation lead to a model by which the edge dislocation array could move continuously with the diffusion front by a glide mechanism.⁽⁵⁾ According to this model an edge dislocation parallel to the surface is generated by recombination of two gliding dislocations with inclined Burgers vectors. The model requires that the glide planes of the two combining dislocations intersect along a line that is parallel to the surface and at right angles to the Burgers vector of the edge dislocation that is being formed. The model is particularly attractive for the {100} surface orientation because the planes of glide can be the {111} type which is the normally observed slip plane for silicon. It is not equally as attractive for the {110} or {111} surface orientation because the plane of glide motion can not be {111}. In the {110} case glide must be on planes of the type {100} and for {111} surface orientation glide must be on {113}. Neither of these are normal slip planes for silicon. Of course it is possible for a dislocation to follow {100} or {113} macroscopically by gliding alternately on two {111} planes. The more frequent the change of slip plane the more it would appear that slip had actually taken place on {100} or {113}. Therefore the glide mechanism is most probable for {100} foils and least likely for {111} foils.

The observations are consistent with this prediction. Dislocations with inclined Burgers vectors that join to form one of the edge dislocations of the main accommodation array were often seen in {100} specimens but were rarely seen in {111} specimens. The arrangement and curvature of individual dislocation segments in specimens of the

latter orientation suggest that motion is primarily by climb. The {110} case is not comparable to the other two because the accommodation array can not be formed entirely of edge dislocations with Burgers vectors parallel to the surface. Many dislocations with Burgers vectors inclined to the surface are necessarily present in the array. Cases were observed such as at B in Fig. 8 where two of these seem to be combining to form a length of edge dislocation, perhaps by glide on {100}. However, as in the {111} specimens, most of the edge dislocations with Burgers vectors parallel to the surface seemed to have moved in by climb. The {110} case was also unique in that some dislocations with the inclined Burgers vectors glide on the inclined (111) and (11 $\bar{1}$) slip planes to a depth much greater than the main part of the accommodation array. Examples are shown in Fig. 9 which is a foil prepared at the level of the p-n junction. In {111} specimens few if any dislocations were found at this level.

Because the stress necessary to cause glide is almost certainly less than the stress necessary to produce climb at a comparable rate at the diffusion temperature, the results suggest that the solute contraction stresses may be more completely relaxed in {100} and {110} specimens than they are in {111} specimens.

CONCLUSIONS

1. The boron and phosphorus diffusion treatments normally employed in device manufacture result in the motion of dislocations in the surface layers so as to relax the solute contraction stresses.
2. After completion of the diffusion treatment the maximum density of dislocations is found at the depth where the remaining concentration gradient is the steepest.
3. Regardless of the orientation of the surface into which diffusion takes place the dislocation array lies approximately parallel to this surface and is composed primarily of edge dislocations having Burgers vectors which are as nearly parallel as possible to the surface.
4. Although strong indications were found previously in specimens with {100} surfaces that edge dislocations parallel to the surface move into the crystal by a glide mechanism, this is not the case for {110} or {111} surfaces. In these cases edge dislocations appear to move in nonconservatively, by climb.

ACKNOWLEDGEMENTS

We should like to acknowledge ITT Shockley Laboratory of Palo Alto and Paul Van Loon for performing the diffusion and sectioning of the silicon wafers.

The continued financial support of the U. S. Atomic Energy Commission is gratefully acknowledged.

LIST OF FIGURES

Fig. 1 Solute profile (Concentration vs Depth) obtained by sectioning of (111) oriented boron diffused wafer. The levels examined by transmission electron microscopy are indicated on the curve.

Fig. 2 Dislocation network observed at level 3b in a (111) oriented boron diffused wafer. The dislocations are steeply inclined to the foil surface as indicated by the dotted contrast.

Fig. 3 Stereo pair of typical area at level 3b (maximum concentration gradient) in a boron diffused (111) wafer. The dislocations are distributed in a three dimensional network rather than as a planer array. Many dislocations are steeply inclined and traverse the foil from top to bottom.

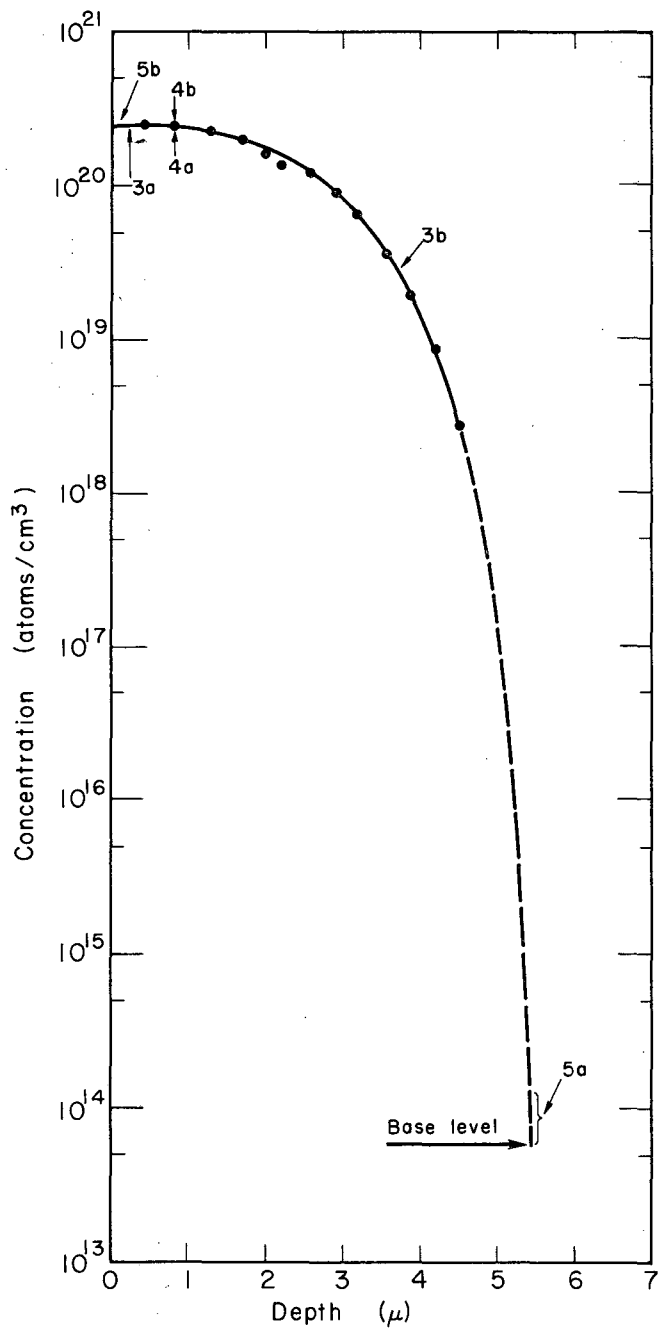
NOTE - To obtain a stereo image, stereo glasses should be placed approximately 6 inches above and centered on the micrographs. The glasses may then be slightly rotated until the two black dots and the dislocation images are superimposed.

Fig. 4 Identical area to that shown in Fig. 3 with Burgers vectors assigned to all the dislocation segments. They are indicated by short lines parallel to their projections onto the (111) foil plane. The six possible projections are indicated by the tetrahedron. Most dislocations are near edge orientation and have one of the three Burgers vectors that are parallel to the diffusion front. Those dislocation lines that have one of the three inclined Burgers vectors are indicated by lines with arrows.

- Fig. 5 Diffusion induced dislocations that have formed near the surface in a $\{111\}$ phosphorus diffused wafer. The dislocations are in edge orientation and have Burgers vectors that are in the (111) plane parallel to the surface. At A, B, and C dislocation half loops corresponding to two of the three coplanar Burgers vectors have climbed into the wafer and have come close enough to begin to interact. At D, E, F and G short segments having the third Burgers vector have been formed. Surface precipitates were also observed.
- Fig. 6 Stereo pair corresponding to Fig. 5. The dislocation half loops appear to have climbed into the crystal.
- Fig. 7 Stereo pair of diffusion induced dislocation network in $\{110\}$ oriented wafer.
- Fig. 8 Indexed Burgers vectors of area shown in stereo view in Fig. 7. The long dislocations in the $[001]$ direction have their Burgers vectors parallel to the (110) plane of diffusion e.g. $a/2 [\bar{1}10]$ and are in predominantly edge orientation. The inclined Burgers vectors are represented by lines drawn parallel to the projection of their Burgers vector in the (110) plane. The hexagonal network consists of both types. The etched area in the lower left hand corner contains precipitation on the perpendicular $\{111\}$ planes.
- Fig. 9 Diffusion induced dislocations with inclined Burgers vectors observed at a depth approximately the same as that of the pn junction.

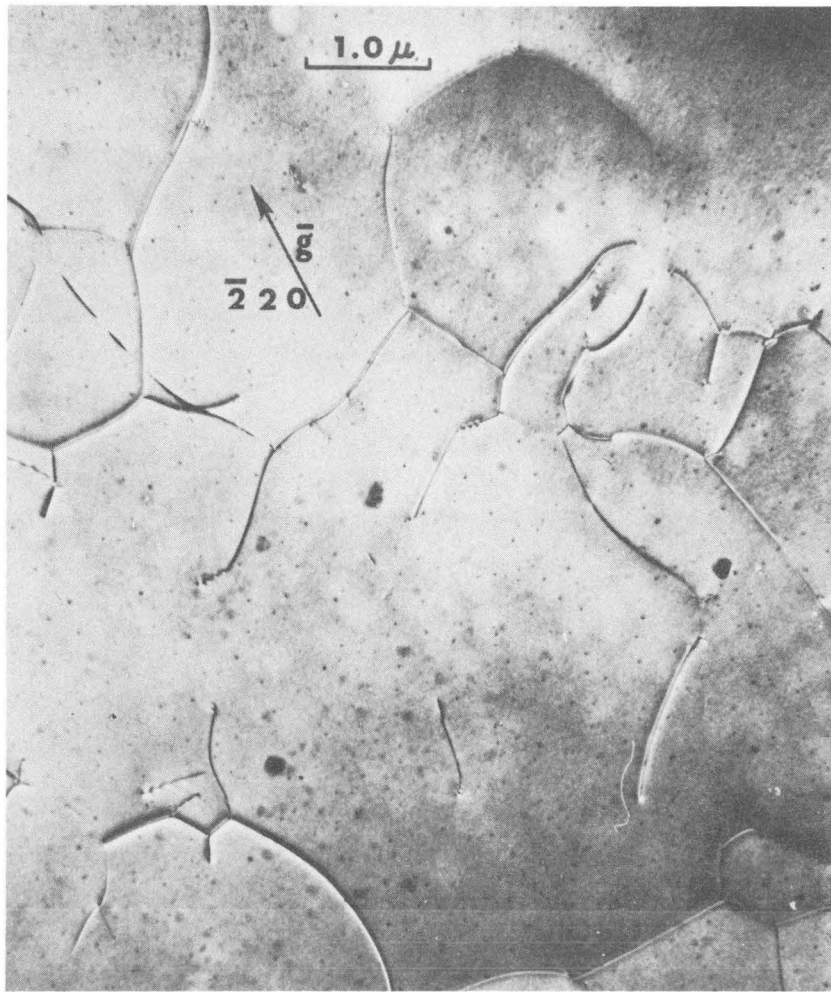
REFERENCES

1. Y. Sato, H. Arata, Jap. Journal Appl. Physics 3, 511 (1964).
2. S. Prussin, J. Appl. Physics, 32, 1876 (1961).
3. G. H. Schwuttke and H. J. Queisser, J. Appl. Physics, 33, 1540 (1962).
4. R. J. Jaccodine, Appl. Physics Letters, 4, No. 114 (1964).
5. J. Washburn, G. Thomas and H. J. Queisser, J. Appl. Physics, 35, 1909 (1964).
6. M. L. Joshi and F. Wilhelm, J. of Electrochem Soc., 112, 185 (1965).
7. E. Tannenbaum, Solid State Electronics, 2, 123 (1961).
8. R. H. Finch, H. J. Queisser, G. Thomas and J. Washburn, J. Appl. Physics, 34, 406 (1963).
9. E. Levine, W. L. Bell, G. Thomas, J. Appl. Physics., 37, 2141 (1966).
10. P. Schmidt and R. Stickler, J. Electrochem Soc., 111, 1188 (1964).



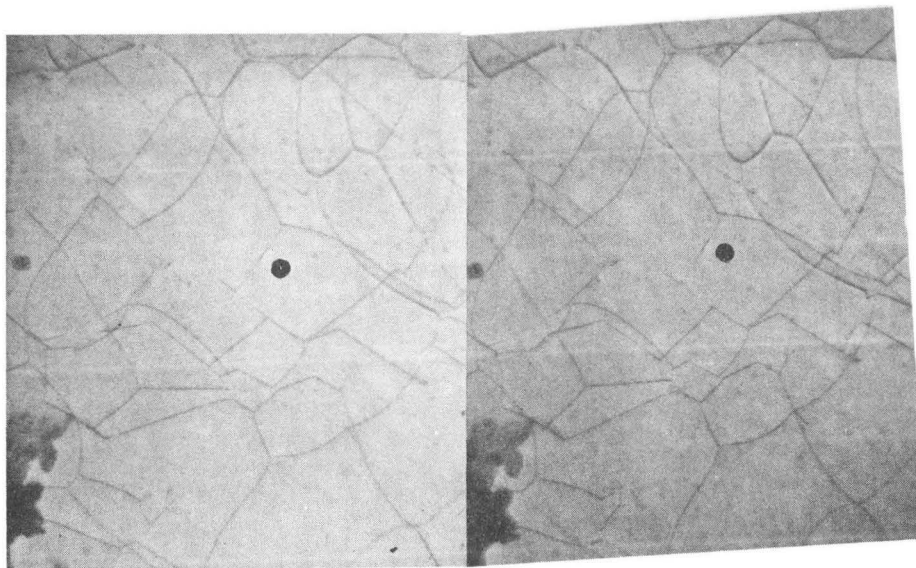
MUB-11074

Fig. 1



ZN-5698

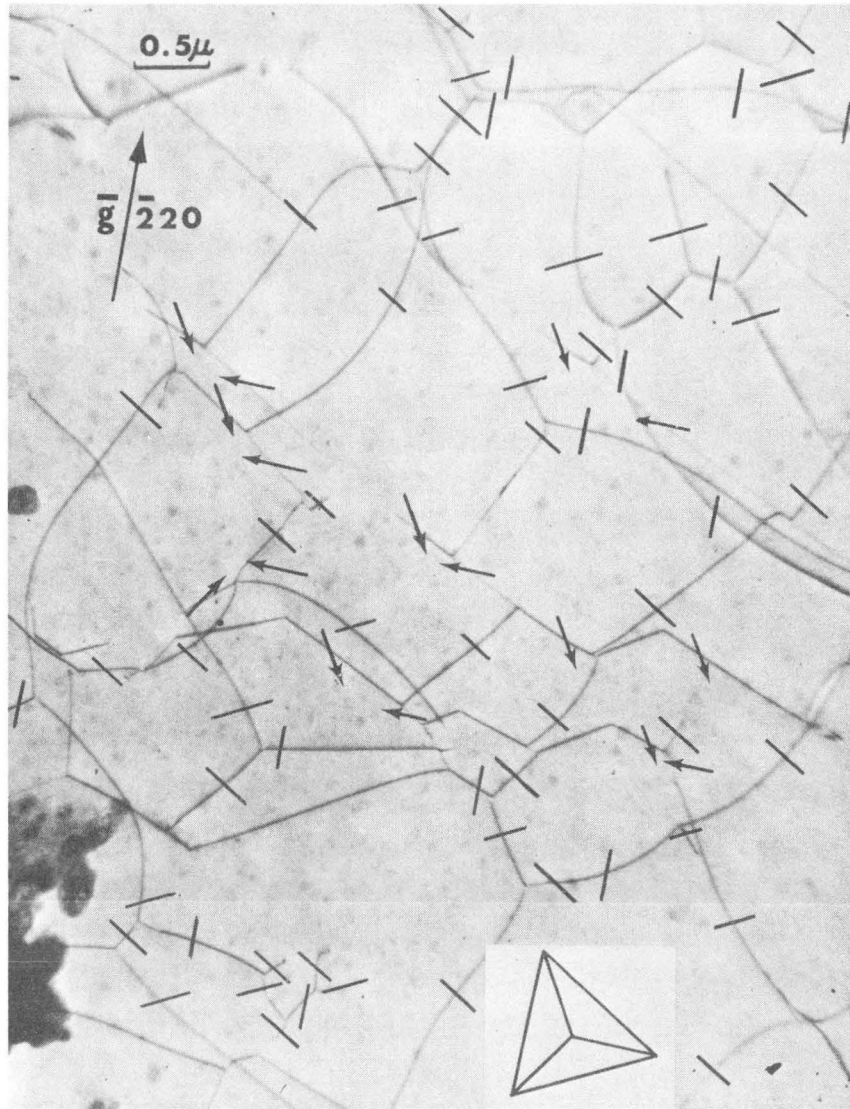
Fig. 2



μ

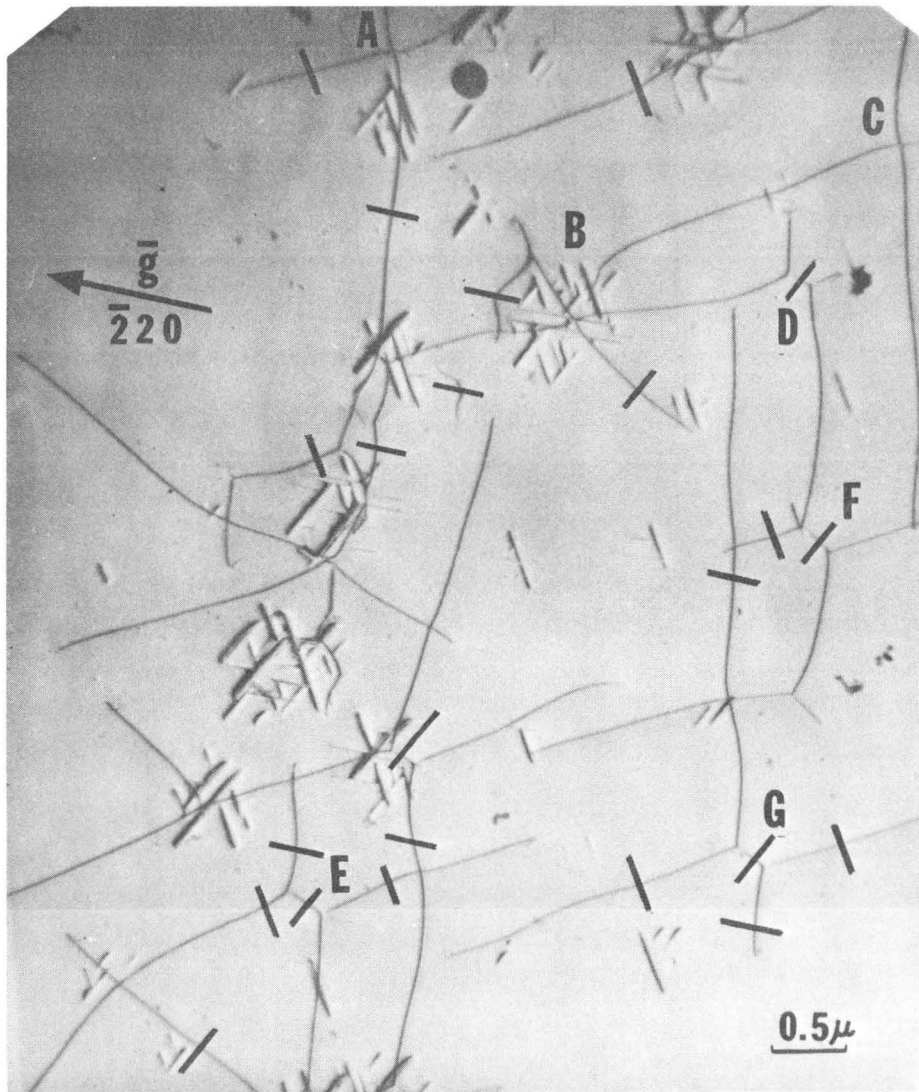
ZN-5703

Fig. 3



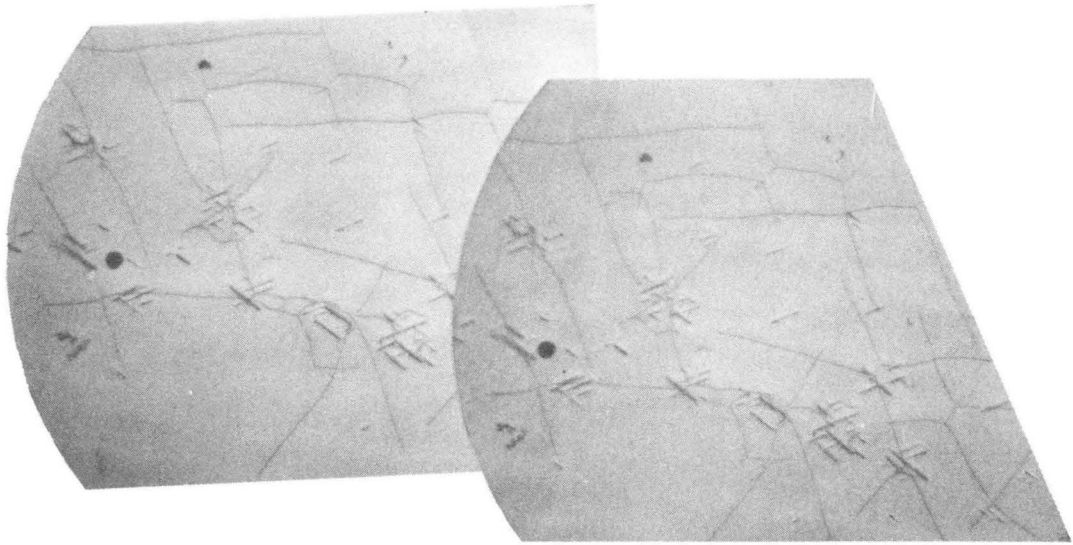
ZN-5699

Fig. 4



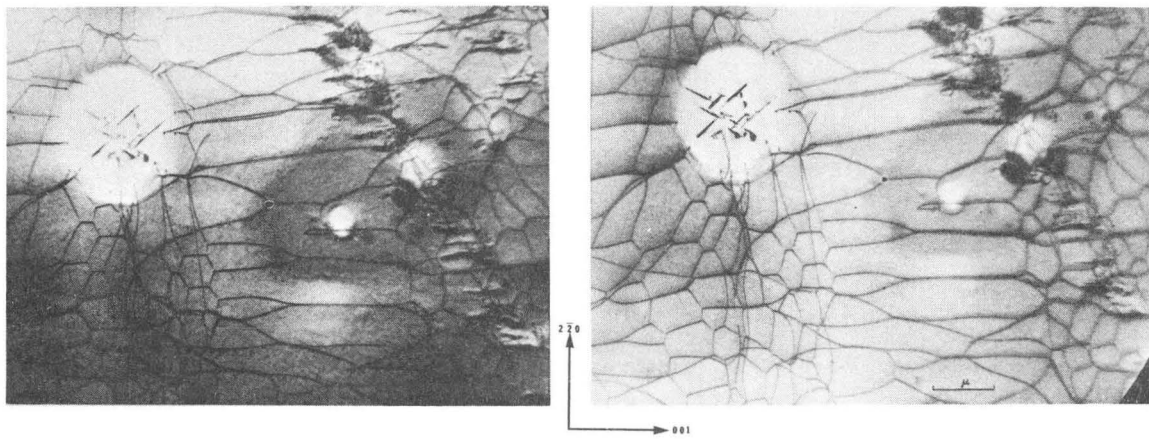
ZN-5700

Fig. 5



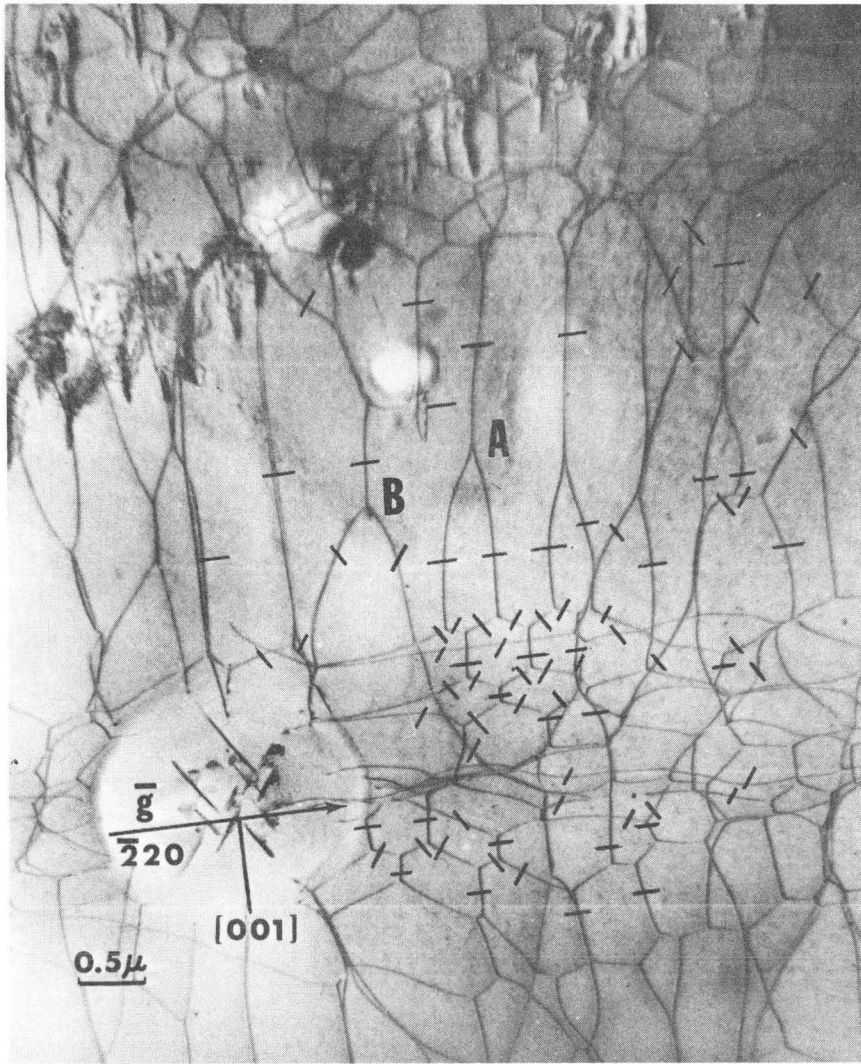
ZN-5704

Fig. 6



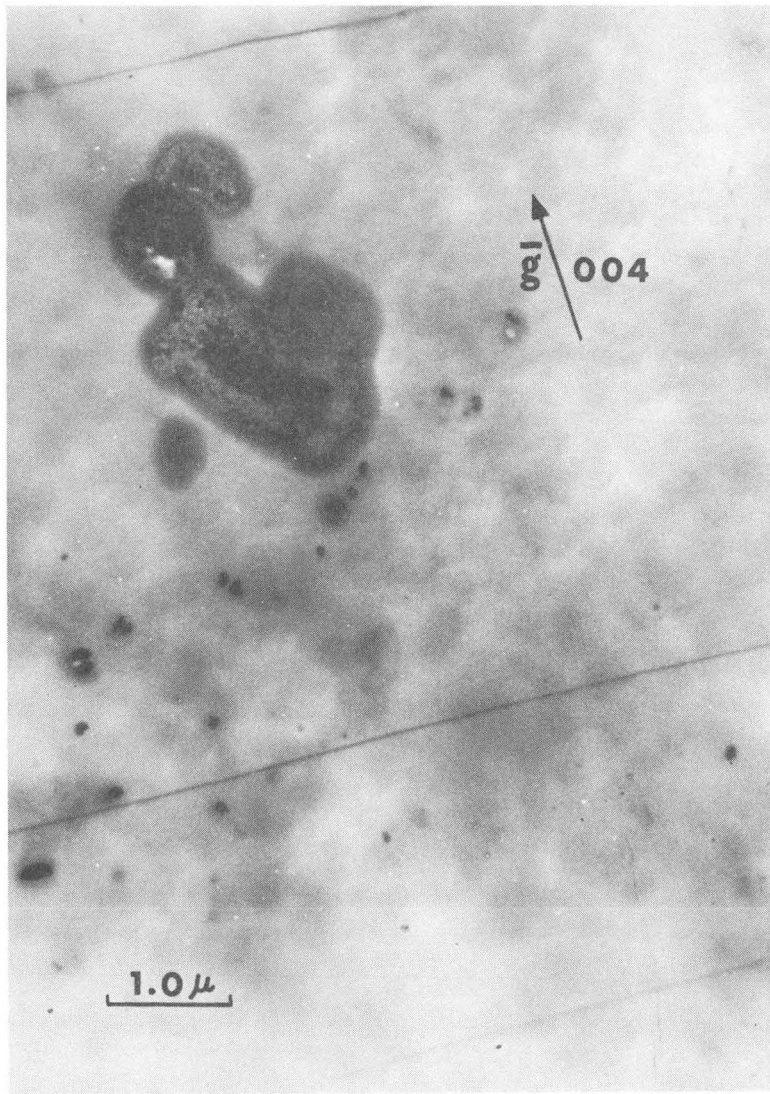
ZN - 5705

Fig. 7



ZN-5701

Fig. 8



ZN-5702

Fig. 9

This report was prepared as an account of Government sponsored work. Neither the United States, nor the Commission, nor any person acting on behalf of the Commission:

- A. Makes any warranty or representation, expressed or implied, with respect to the accuracy, completeness, or usefulness of the information contained in this report, or that the use of any information, apparatus, method, or process disclosed in this report may not infringe privately owned rights; or
- B. Assumes any liabilities with respect to the use of, or for damages resulting from the use of any information, apparatus, method, or process disclosed in this report.

As used in the above, "person acting on behalf of the Commission" includes any employee or contractor of the Commission, or employee of such contractor, to the extent that such employee or contractor of the Commission, or employee of such contractor prepares, disseminates, or provides access to, any information pursuant to his employment or contract with the Commission, or his employment with such contractor.

